

# An evaluative study on ESO and SIMP for optimising a cantilever tie-beam

C. S. Edwards · H. A. Kim · C. J. Budd

Received: 12 June 2006 / Revised manuscript received: 23 January 2007 / Published online: 14 March 2007  
© Springer-Verlag 2007

**Abstract** We examine both the evolutionary structural optimisation (ESO) and solid isotropic microstructure with penalisation (SIMP) methodologies by investigating a cantilever tie-beam. Initially, both ESO and SIMP produce designs with higher objective function values relative to a previously published ‘intuitive’ design. However, after careful investigation of the numerical parameters such as the initial design domain and the mesh size, both methods obtain designs that have lower objective function values relative to the intuitive design. Thus, a clearer understanding of the numerical parameters and their influence on optimisation methods is achieved.

**Keywords** Topology optimisation · Evolutionary structural optimisation (ESO) · Solid isotropic microstructure with penalisation (SIMP)

## 1 Introduction

Topology optimisation is a method for finding the optimal material distribution within a fixed design do-

main  $\Omega$ . An optimum can be defined by various objective functions such as minimum compliance or a fully stressed design. The design domain is usually discretised using finite elements with the existence of the elements being the design variable.

Inherent to many topology optimisation methods is a numerical instability, which results in chequerboard patterns. There has been much research into the chequer board phenomenon including Díaz and Sigmund (1995) who find the stiffness of a chequerboard pattern to be higher and therefore favoured over its continuous equivalent. Also, Jog and Haber (1996) find chequerboard patterns to be a result of mixed finite element models where the existence of an element is piecewise constant, whereas the displacement of an element is piecewise linear. There have been various methods developed for dealing with chequerboard patterns including the use of higher order elements (Jog and Haber 1996), perimeter constraints (Haber et al. 1996) and filtering to smooth the sensitivity distribution (Sigmund 1994). A review of numerical instabilities and how to deal with them can be found in Sigmund and Petersson (1998).

Solving optimisation problems with discrete design variables is generally considered to be more difficult than with continuous design variables (Sigmund and Petersson 1998). Thus, a typical method used to solve topology optimisation problems is to relax the layout design variable by introducing intermediate states for an element that are between solid and void. This new layout design variable is analogous to the continuous density of the element. However, this density is somewhat artificial, and a design with a continuous density distribution cannot be manufactured. Therefore, the intermediate densities are penalised using a power-law to

---

C. S. Edwards (✉) · H. A. Kim  
Department of Mechanical Engineering, University of Bath,  
Bath BA2 7AY, UK  
e-mail: C.S.Edwards@bath.ac.uk

H. A. Kim  
e-mail: H.A.Kim@bath.ac.uk

C. J. Budd  
Department of Mathematical Sciences, University of Bath,  
Bath BA2 7AY, UK  
e-mail: C.J.Budd@bath.ac.uk

give them low stiffness, thus, producing a near discrete solution. This approach is referred to as solid isotropic microstructure with penalisation (SIMP) (Bendsøe 1989; Rozvany and Zhou 1991, presented in 1990; Rozvany et al. 1992; Bendsøe and Sigmund 2003).

Reitz (2001) has shown that there exists a discrete solution to the SIMP problem if a sufficiently high penalisation is used. The proof contains the following assumptions: there is only one constraint (volume), the objective function is continuously differentiable and its derivatives are negative and bounded and also that there exists a unique discrete solution. Subsequently, Martínez (2005) relaxes these assumptions by showing, for example, the solution does not necessarily need to be unique. However, using high values of penalisation can result in local minima because the penalised design problem is not convex (Petersson and Sigmund 1998). Thus, continuation or homotopy methods are used to increase the likelihood of obtaining a global minimum (Allgower and Georg 1990).

An alternative topology optimisation method is evolutionary structural optimisation (ESO) (Xie and Steven 1993, 1997). ESO slowly removes redundant material to evolve the structure to an optimum. Redundant material is characterised by low local sensitivity values, for example, strain energy, calculated using finite element analysis (FEA).

Unlike SIMP, ESO was originally developed as a heuristic method derived from engineering intuition. The subsequent research efforts over the following decade demonstrated numerically that ESO generally finds an optimal solution (Xie and Steven 1997). Noting that the ESO solution agreed well with the Michell structure where the compliance–volume (C–V) product is minimum, Tanskanen (2002) recently proposed that this reflects the objective function of the ESO method. It was outlined that the strategy of removing elements with low strain energy is analogous to sequential linear programming and leads to a constant strain energy distribution, hence, minimising the C–V product.

Zhou and Rozvany (2001) introduced a numerical example where ESO's strategy of removing the elements increased the total compliance by a factor of 10. This was because the element removal under consideration fundamentally changed the way the loads were transmitted, and hence, the structure evolved to a sub-optimal solution.

Inspired by such an interesting problem, the current paper further investigates the test problem of Zhou and Rozvany (2001). The aim of this paper is to compare the optimisation ability of SIMP and ESO by considering the effects of discretisation, penalisation and initial design.

In the following section, we briefly outline the optimisation problem formulations for the SIMP and ESO strategies. Section 3 defines the test example used for this investigation. The influence of mesh density and the initial design domain is analysed for ESO and then SIMP in the subsequent sections, which is followed by the conclusions.

## 2 Problem formulations for the topology optimisation methods

### 2.1 The SIMP approach

The SIMP formulation is based on the continuous problem of minimising the total compliance  $C$  parameterised by a vector of coordinates  $\xi \in \Omega$  with a volume constraint  $V_c$ ,

$$\left. \begin{array}{l} \min : C \\ \text{subject to : } V \leq V_c \end{array} \right\}. \quad (1)$$

In the finite element environment, a set of  $n$  elements over  $\xi \in \Omega$  is used to represent a structure. The design variable  $x(\xi)$  is the presence of material, which is discrete. This is relaxed such that it is continuous over  $(0, 1]$ . The intermediate values are penalised by a power-law (typically, power  $p \sim 3$ ) to steer the solution to a discrete topology.

The optimisation problem is constrained to satisfy the elastic equilibrium equation (2) for global stiffness matrix  $\mathbf{K}$  and load vector  $\mathbf{f}$ .

$$\mathbf{K}\mathbf{u} = \mathbf{f} \quad (2)$$

The element stiffness  $\mathbf{K}_i$  can be written in terms of  $\mathbf{x} = \{x_1, x_2, \dots, x_n\}$  as

$$\mathbf{K}_i = x_i^p \mathbf{K}_0, \quad (3)$$

where  $x_i \in (0, 1]$  and  $\mathbf{K}_0$  is the element stiffness constant with  $x_i = 1$ . Using the above notation for symmetric  $\mathbf{K}$ , the total compliance is written as

$$C_p(\mathbf{x}) = \mathbf{f}^T \mathbf{u} = \mathbf{u}^T \mathbf{K} \mathbf{u} = \sum_i x_i^p \mathbf{u}_i^T \mathbf{K}_0 \mathbf{u}_i. \quad (4)$$

The SIMP optimisation problem is thus defined as

$$\left. \begin{array}{l} \min_{\mathbf{x}} : C_p(\mathbf{x}) = \sum_{i=1}^n x_i^p \mathbf{u}_i^T \mathbf{K}_0 \mathbf{u}_i \\ \text{subject to : } V(\mathbf{x}) \leq V_c \\ \quad : \mathbf{0} < x(\xi)_{\min} \leq x(\xi) \leq 1 \end{array} \right\}, \quad (5)$$

where  $x(\xi)_{\min}$  is a vector of minimum densities to avoid singularities and  $V(\mathbf{x})$  is the current total material volume (Bendsøe and Sigmund 2003).

SIMP has a well-defined objective function, and the optimisation problem in (5) can be tackled using a variety of sophisticated algorithms such as the method of moving asymptotes (MMA) algorithm (Svanberg 1987).

The penalisation of SIMP causes the design space to be non-convex, and thus, there may exist local minima. When high values of  $p$  are used, local minima are often produced rather than the global minimum. Thus, a continuation method, like that described by Petersson and Sigmund (1998), is used for such problems. We implement SIMP initially with a penalisation of  $p_{\text{init}} = 1$  until a solution has converged. The penalisation is then increased by 0.5, and the current solution is used as the new initial topology. This process is repeated until the penalisation value gives as discrete solution as possible but does not cause the stiffness matrix  $\mathbf{K}$  to be ill-conditioned.

We implement SIMP in this paper using the MMA algorithm in conjunction with the MATLAB (The Math Works 2004) code in Sigmund (2001).

## 2.2 The ESO approach

ESO optimises a structure by slowly removing the material that has the lowest sensitivity value, such as stress or strain energy  $U$  defined in (6), from the design domain. The sensitivity chosen reflects the objective function of the optimisation problem. It has been proposed that the removal of elements with the lowest strain energy leads to a design with a uniform strain energy distribution (Tanskanen 2002).

$$U_i = \frac{1}{2} \mathbf{u}_i^T \mathbf{K}_i \mathbf{u}_i. \quad (6)$$

Unlike SIMP, ESO treats the design variable  $x$  as a discrete variable that takes a value of either '1' when an element is present or '0' when completely removed. Thus, the element stiffness  $\mathbf{K}_i$  for ESO, written in terms of the elemental design variable  $x_i$ , is

$$\mathbf{K}_i = x_i \mathbf{K}_0, \quad (7)$$

where  $x_i \in \{0, 1\}$ .

An outline of the ESO algorithm can be summarised as follows:

1. An optimisation problem is defined by specifying the kinematic conditions and the initial design domain, appropriately discretised, in the FE environment.

2. FEA computes the displacement field, and hence, the strain energy of the given design.
3. The elements that satisfy (8) are removed,

$$U_i \leq \text{RR} \cdot U_{\min} \quad (8)$$

where RR is the rejection ratio and  $U_{\min}$  is the minimum elemental strain energy. The rejection ratio controls the optimisation rate and needs to be sufficiently small to do so. Thus, RR is defined empirically and is problem dependent.

4. Steps 2 to 3 are repeated until all elements are removed or the stiffness matrix  $\mathbf{K}$  becomes ill-conditioned. The latter case is what we usually see.
5. Examine the evolutionary history and select the design that has a locally minimum objective function value and/or desirable volume ratio. We, henceforth, refer to the local and global minimum of the iteration history for a single run as the S-history local and S-history single-run-global minimum, respectively.

Tanskanen (2002) shows that removing elements with the lowest strain energy achieves a structure with a minimum compliance–volume product. Thus, an appropriate objective function is the compliance–volume product  $S(\mathbf{x})$ . Using equations (2) and (7), compliance is defined as

$$C(\mathbf{x}) = \sum_i x_i \mathbf{u}_i^T \mathbf{K}_0 \mathbf{u}_i \quad (9)$$

Letting the volume of an element  $j$  be  $v_j$  and for symmetric  $\mathbf{K}$ ,  $S(\mathbf{x})$  is defined as

$$S(\mathbf{x}) = CV = \mathbf{u}^T \mathbf{K} \mathbf{u} V = \sum_i x_i \mathbf{u}_i^T \mathbf{K}_0 \mathbf{u}_i \sum_j x_j v_j. \quad (10)$$

Thus, we can write the optimisation problem as (Tanskanen 2002):

$$\left. \begin{aligned} \min_{\mathbf{x}} : S(\mathbf{x}) &= \sum_i x_i \mathbf{u}_i^T \mathbf{K}_0 \mathbf{u}_i \sum_j x_j v_j \\ : x_i &\in \{0, 1\} \quad i = 1, 2, \dots, n. \end{aligned} \right\}. \quad (11)$$

The ESO algorithm, as described, does not stop once the objective function  $S(\mathbf{x})$  has reached a minimum; it continues to remove elements until either all elements have been removed or the stiffness matrix  $\mathbf{K}$  becomes ill-conditioned. This further removal of elements may lead to S-history local minima with significantly smaller volume than the S-history single-run-global minimum.

One of the main differences in the formulations for ESO and SIMP is the volume. ESO reduces the volume to find the optimum topology solution, whereas SIMP finds the optimum topology solution to the given volume specified a priori. Thus, to make a precise

comparison of the results from ESO with those of SIMP, we will consider the ESO objective function  $S(\mathbf{x})$  and constrain SIMP to the final volume of the ESO solutions. The results are also to be compared with those of Edwards et al. (2006) where ESO was implemented using von Mises stress as opposed to strain energy and SIMP was implemented using the heuristic updating scheme of Bendsøe and Sigmund (2003).

We implement ESO in this paper using an Intel® FORTRAN compiler with the MA57 multi-frontal linear solver (Rutherford Appleton Laboratory 2004). The results from the MA57 linear solver have been validated against MATLAB (The Math Works 2004). MATLAB is then used to produce the graphical images.

### 2.3 Numerical instabilities and filtering

Topology optimisation can often exhibit an instability for which the resulting topology contains a checkerboard pattern of active and removed elements or of high- and low-density elements. It has been established that the appearance of these checkerboard patterns is a numerical instability and does not represent an optimal design (Sigmund 1994; Díaz and Sigmund 1995; Jog and Haber 1996; Kim et al. 2000).

A popular heuristic treatment for preventing checkerboard formations is checkerboard filtering or local smoothing of sensitivities similar to low pass filtering in signal and image processing. This filtering technique works by smoothing local sensitivities after analysis and then these smoothed sensitivities are used to modify and optimise the design.

The filter implemented in this investigation is the Bartlett filter, which takes a weighted average of sensitivities within a specified region (Sigmund 1994). This specified region is defined by the parameter  $r_{\min}$ , the radius taken from the centre of the element  $i$ .

$$\hat{S}_i = \frac{1}{x_i \sum_j \hat{H}_j} \sum_j \hat{H}_j x_j S_j, \quad (12)$$

where  $\hat{S}_i$  is the filtered sensitivity of element  $i$ ,  $S_i$  is the original sensitivity of element  $i$  and  $\hat{H}$  is the weighting factor for all enclosed elements  $j$  within  $r_{\min}$  and is determined based on the distance between elements  $i$  and  $j$  (13).

$$\hat{H}_j = r_{\min} - \text{dist}(i, j). \quad (13)$$

### 3 Tie-beam test problem

The tie-beam test problem was presented in Zhou and Rozvany (2001) with the aim of highlighting the possible shortcomings of ESO. This tie-beam is used in this investigation for further examination of the ESO method by comparing the solutions obtained with those of the well-established SIMP method.

The test problem is an L-shaped clamped beam with a roller support at the top of the vertical section of the beam, which is referred to as the vertical tie (Fig. 1). There is a *single* load case consisting of a vertical tensile load of intensity  $L_y = 1.0$  and a horizontal compressive load of intensity  $L_x = 2.0$ . The Young's modulus ( $E$ ) is specified as 1 and the Poisson's ratio ( $\nu$ ) is 0. This test problem is modelled using  $n = 100$  four node plane stress elements with unit thickness (Zhou and Rozvany 2001). This mesh, as specified in the literature, is particularly coarse, as the width of the vertical tie is only one element.

With the objective of optimisation defined as minimising compliance, Zhou and Rozvany (2001) suggest the design of Fig. 2 as an 'intuitive optimal solution' with a total compliance of  $C(\mathbf{x}) = 1,117$ , a volume of  $V(\mathbf{x}) = 40$  and  $S(\mathbf{x}) = 44,684$ . This design is, henceforth, referred to as the "tie-beam solution," as it has no proof of optimality.

In addition to the tie-beam solution of Fig. 2, there exists a sub-optimal design with both larger volume and compliance than the intuitive design. We refer to this sub-optimal design as the "cantilever solution" because the roller support at the top is removed producing a system that behaves like a cantilevered beam. An example of a cantilever solution is illustrated in Fig. 3.

Zhou and Rozvany (2001) used elemental strain energy as the sensitivity for ESO. When Fig. 1 is analysed using FEA, the element with the lowest strain energy is identified to be element 'A'. This strain-energy-based ESO algorithm therefore removes element 'A' in the first iteration, and the present algorithm does not allow re-admission of the element. The removal of element 'A' detaches the beam from the roller support, and the

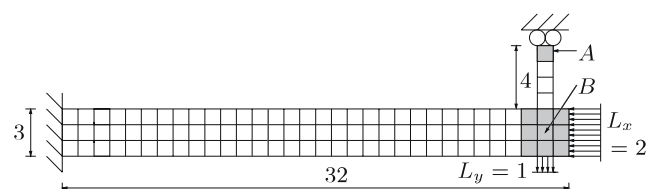


**Fig. 1** Test problem with a coarse mesh (Zhou and Rozvany 2001) having  $V(\mathbf{x}) = 100$ ,  $C(\mathbf{x}) = 390$ ,  $S(\mathbf{x}) = 38,986$  and the load intensities  $L_x$  and  $L_y$  are defined per unit area

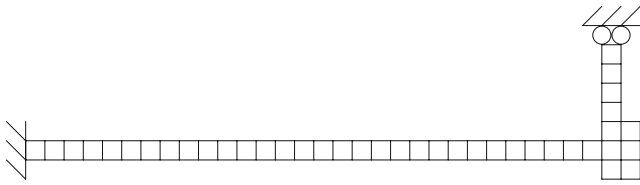


**Fig. 2** Tie-beam solution with  $V(\mathbf{x}) = 40$ ,  $C(\mathbf{x}) = 1,117$  and  $S(\mathbf{x}) = 44,684$

beam effectively becomes a cantilever beam, transmitting the vertical load as bending.

The change in load transmission to bending increases the ESO objective function from  $S(\mathbf{x}) = 38,986$  to  $S(\mathbf{x}) = 460,523$ . However, because ESO is not minimising compliance  $C(\mathbf{x})$ , rather the compliance–volume product  $S(\mathbf{x})$ , it is clear that the tie-beam solution of Fig. 2 is not a minimum design of  $S(\mathbf{x})$ . The tie-beam solution is not a minimum of  $S(\mathbf{x})$  because  $S(\mathbf{x})$  for the initial design domain is 13% lower than it is for the tie-beam solution.

#### 4 Application of ESO

In this section, the previously described test problem is modified to have a larger initial design domain and to finer computational meshes. For consistency, all compliance calculations are made using the refined mesh. The results of applying ESO to the revised test problems are presented.

##### 4.1 Investigation of ESO using a coarse mesh with a rectangular initial design domain

To investigate the effects of the initial design domain on the test problem, the initial design domain is modified to a rectangle containing the original problem and is shown in Fig. 4.

We apply ESO with the filtering technique of Section 2.3 to the ESO sensitivities by taking a weighted average of elemental strain energy. We use  $r_{\min} = 1.05$ , which is particularly small because the mesh is coarse. Experience has shown that a very small rejection ratio is also required to ensure slow material removal, and therefore,  $RR = 1.03$  is used. Using these optimisation

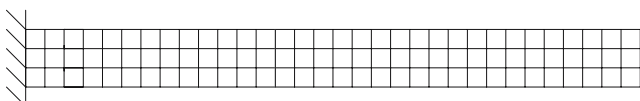


**Fig. 3** An example of a cantilever solution where  $V(\mathbf{x}) = 96$ ,  $C(\mathbf{x}) = 4,387$  and  $S(\mathbf{x}) = 421,180$

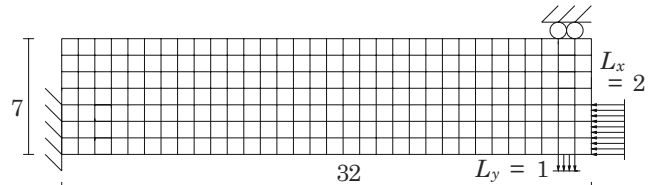


**Fig. 4** Rectangular initial design domain encompassing original design domain with  $V(\mathbf{x}) = 224$ ,  $C(\mathbf{x}) = 283$  and  $S(\mathbf{x}) = 63,430$

parameters, an S-history single-run-global minimum is reached after 97 iterations.

The material design  $\mathbf{x}$  of the S-history single-run-global minimum is illustrated in Fig. 5 and has a volume of  $V(\mathbf{x}) = 101$ . The original initial design domain of Fig. 1 has a similar volume to this S-history global solution with  $V(\mathbf{x}) = 100$ . However, the objective function for the S-history single-run-global minimum is  $S(\mathbf{x}) = 39,997$ , which is 3% higher than for the original initial design domain where  $S(\mathbf{x}) = 38,986$ . The difference in  $S(\mathbf{x})$  is caused through the inability of ESO to replace previously removed elements if required.

In comparison to the tie-beam solution of Fig. 2, the S-history single-run-global minimum has lower  $S(\mathbf{x})$  and  $C(\mathbf{x}) = 396$  but higher  $V(\mathbf{x})$  because  $S(\mathbf{x}) = 44,684$ ,  $C(\mathbf{x}) = 1,117$  and  $V(\mathbf{x}) = 40$  for the tie-beam solution. Thus, the design of Fig. 5 has a more efficient use of material, but more weight, compared to the tie-beam solution.

Figure 6 shows the iteration history of the objective function  $S(\mathbf{x})$  and the volume  $V(\mathbf{x})$ . The S-history single-run-global minimum is achieved at ‘c’ (Fig. 5). However, the volume continues to decrease because ESO does not have a stopping criterion and the material continues to be removed. Thus, the vertical tie becomes detached, and the objective function increases significantly. The detachment of the vertical tie occurs only two iterations after the S-history single-run-global minimum (c) is achieved.

To understand why ESO cannot further reduce the volume of the test problem, we investigate the appropriateness of the given mesh size below.



**Fig. 5** S-history single-run-global minimum design of  $S(\mathbf{x})$  (c) by ESO for the rectangular initial design domain.  $V(\mathbf{x}) = 101$ ,  $C(\mathbf{x}) = 396$  and  $S(\mathbf{x}) = 39,997$ . The compliance  $C(\mathbf{x})$  is calculated using the refined mesh of Fig. 7



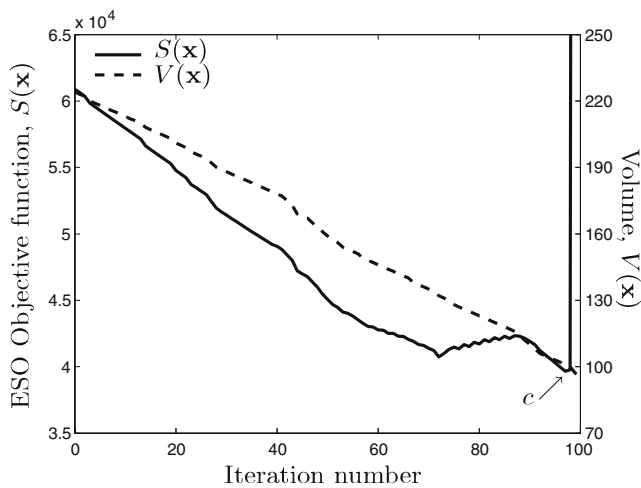


**Fig. 6** Iteration history for the ESO objective function when applied to a rectangular initial design domain. The sharp increase around ‘c’ represents the point where the vertical tie is detached

#### 4.2 Investigation of mesh size

To understand why the ESO algorithm evolves the structure towards the cantilever beam, we return to the original initial design domain of Fig. 1 and the optimality criterion of constant strain energy.

The tie-beam configuration primarily transmits the applied loads axially. Thus, we simplify the configuration into a pin-jointed truss and ignore the negligible bending stress in region ‘B’ marked in Fig. 1. The simplified system transmits the total horizontal load  $F_x$  and the total vertical load  $F_y$  completely to the horizontal beam and the vertical tie, respectively.

Let  $A_x$  be the cross-sectional area to which  $F_x$  is applied and  $A_y$  be the cross-sectional area of the vertical tie to which  $F_y$  is applied. Then the mean strain energy per element in the vertical tie is

$$\frac{F_y^2 d_y}{2 A_y n_y E} \quad (14)$$

where  $d_y = 4$  is the length of the vertical tie and  $n_y$  is the number of elements in the vertical tie. Also, the horizontal beam has a mean strain energy per element of

$$\frac{F_x^2 d_x}{2 A_x n_x E} \quad (15)$$

where  $d_x = 32$  is the length of the main beam and  $n_x$  is the number of elements in that beam. Thus, for constant strain energy, we must have

$$\frac{F_x^2 d_x}{2 A_x n_x E} = \frac{F_y^2 d_y}{2 A_y n_y E} \quad (16)$$

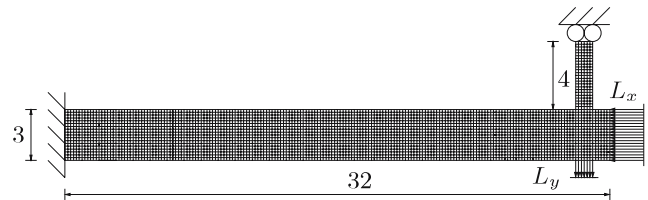


**Fig. 7** Original initial design domain with a refined mesh having  $V(\mathbf{x}) = 100$ ,  $C(\mathbf{x}) = 390$ ,  $S(\mathbf{x}) = 38,986$

The test problem has a horizontal load intensity of  $L_x = 2$  and a vertical load intensity of  $L_y = 1$ . These load intensities are measured in load per unit area where each element is of unit size. In the horizontal beam where the total cross-sectional area is 3 units, the total horizontal applied load is  $F_x = 6$ , and in the vertical tie, the total vertical applied load is  $F_y = 1$ . Therefore, the required cross-sectional area of the vertical tie for constant strain energy can be obtained as

$$\frac{6^2 \cdot 32}{2 \cdot 3 \cdot 96 \cdot 1} = \frac{1^2 \cdot 4}{2 A_y \cdot 4 \cdot 1} \Rightarrow A_y = \frac{1}{4}. \quad (17)$$

The required element size for the vertical tie is one fourth of the original element size. It can, therefore, be deduced that the vertical tie is eliminated in the early stages of optimisation because the vertical tie has a mesh that is too coarse to have constant strain energy. To compare the results with those in Edwards et al. (2006), the mesh is refined such that the element size is one sixth of the original size.

#### 4.3 Investigation of ESO using a refined mesh with the original initial design domain

Applying the mesh refinement gives the initial design domain of Fig. 7, which is the same as Fig. 1 but with  $n = 3,600$  plane stress elements. We optimise this test problem with the refined initial design domain via ESO again using  $RR = 1.03$ . However, the filter we apply is  $r_{\min} = 2.5$  of the new element size. This is equivalent to  $r_{\min} = 0.42$  of the original element size. The filter size is different from that used with the coarse mesh of the original initial design domain because an appropriate



**Fig. 8** Design for the S-history local minimum (d) by ESO on a refined initial design domain with  $V(\mathbf{x}) = 39$ ,  $C(\mathbf{x}) = 1,058$  and  $S(\mathbf{x}) = 41,699$

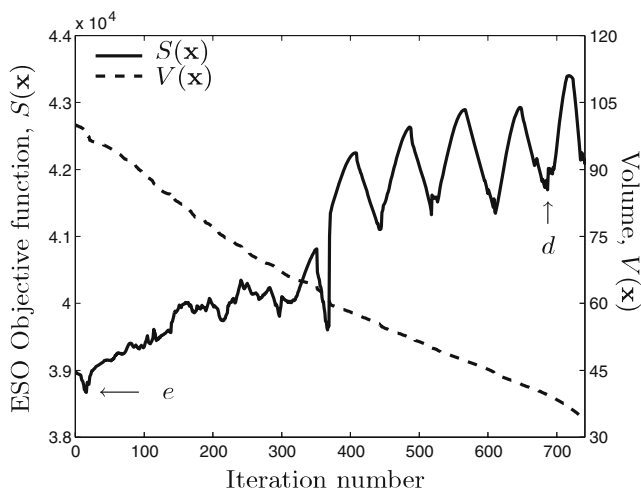


**Fig. 9** Iteration history of  $S(\mathbf{x})$ , for ESO applied to the refined initial design domain

filter size for the new element size is smaller than the size of an original element.

To compare with the tie-beam solution, we select a design with a volume  $V(\mathbf{x}) \approx 40$ . Figure 8 presents a design with a volume of  $V(\mathbf{x}) = 39$ ,  $C(\mathbf{x}) = 1,058$  and  $S(\mathbf{x}) = 41,699$ . Comparing this design with the tie-beam solution of Fig. 2, we find this S-history local minimum has the lower volume, compliance, and thus, volume-compliance product  $S(\mathbf{x})$ . We note that this design of Fig. 8 exhibits a grillage-like structure at the beam-tie intersection and that the vertical tie remains.

Figure 9 shows the graph of the objective function  $S(\mathbf{x})$  and volume  $V(\mathbf{x})$ . The S-history local minimum of Fig. 8 is marked 'd' at iteration 687. The graph clearly shows the volume decreases after the S-history global minimum has been achieved at 'e', and thus, there exist other S-history local minima in between 'd' and 'e'.

The S-history single-run-global minimum occurs after only 16 iterations and is illustrated in Fig. 10. The compliance  $C(\mathbf{x}) = 392$  and the objective function  $S(\mathbf{x}) = 38,671$ . However, the volume has only been reduced by 1% to  $V(\mathbf{x}) = 99$ . Thus, in terms of ESO, this design has the lowest  $S(\mathbf{x})$  of all designs so far, including the tie-beam solution of Fig. 2.

The two-tie configuration design, illustrated in Fig. 10, is favoured by ESO because there exists a local



**Fig. 10** Design for the S-history single-run-global minimum of  $S(\mathbf{x})$  (e) by ESO on a refined initial design domain having  $V(\mathbf{x}) = 99$ ,  $C(\mathbf{x}) = 392$ ,  $S(\mathbf{x}) = 38,671$

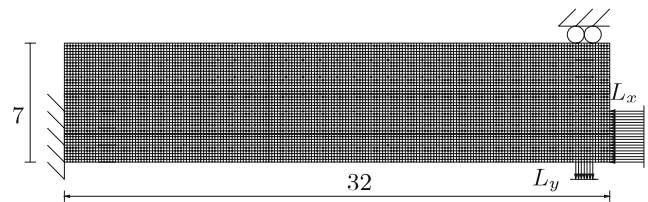


**Fig. 11** Refined rectangular initial design domain encompassing original design,  $V(\mathbf{x}) = 224$ ,  $C(\mathbf{x}) = 283$  and  $S(\mathbf{x}) = 63,430$

strain energy concentration at the re-entrant corners of the main beam where it meets the vertical tie at 'F' for example. This local strain energy concentration increases the elemental strain energy along the boundary, hence, favouring the internal elements for removal. This pattern of element removal, determined by local concentrations, may be considered as a shortcoming of ESO because the severe strategy for the complete removal in ESO exacerbates the numerical issues at the sharp corners.

Edwards et al. (2006) used von Mises stress as the sensitivity for ESO. An objective-history local minimum with volume  $V(\mathbf{x}) \approx 40$ , which has lower compliance than the tie-beam solution of Fig. 2, was obtained. The topology of the objective-history local minimum also contained a grillage-like structure at the beam-tie interface. The objective-history single-run-global minimum obtained in Edwards et al. (2006) also only had a 1% volume reduction, and the vertical tie took the two-tie configuration. Thus, ESO produces consistent results whether von Mises stress or strain energy is used as the sensitivity.

#### 4.4 Investigation of ESO using the refined mesh with a rectangular initial design domain

We continue to investigate by applying ESO to a rectangular initial design domain with the finer mesh such that  $n = 6,064$  (Fig. 11).

As with the coarse mesh of Fig. 4,  $S(\mathbf{x}) = 63,430$  for the rectangular initial design domain, which is higher than  $S(\mathbf{x}) = 44,684$  for the tie-beam solution of Fig. 2. However, the previous design using a refined mesh (Fig. 8) has an even lower  $S(\mathbf{x})$  (compared to the tie-beam solution of Fig. 2). Thus, we expect to achieve a



**Fig. 12** Material distribution for the S-history local minimum (g) when ESO is applied to a refined rectangular initial design domain.  $V(\mathbf{x}) = 43$ ,  $C(\mathbf{x}) = 958$  and  $S(\mathbf{x}) = 41,469$

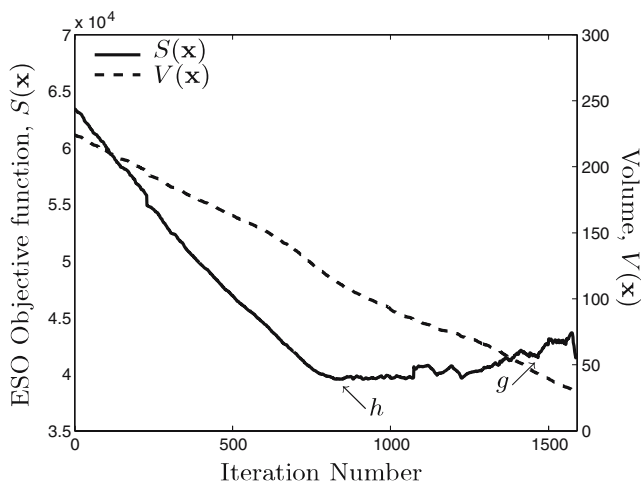


**Fig. 13** ESO iteration history where a refined rectangular initial design domain is used

design similar to that of Fig. 8 rather than of the tie-beam solution of Fig. 2.

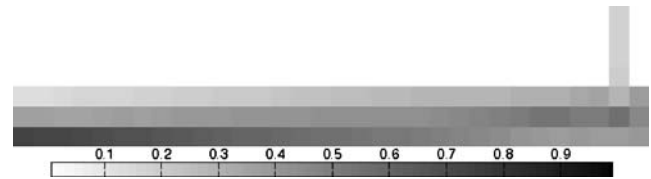
We apply ESO with  $RR = 1.03$  and with a filter of  $r_{\min} = 2.5$  for the refined element size. An S-history local minimum of  $S(\mathbf{x})$  is produced and is illustrated in Fig. 12. The volume for this design is  $V(\mathbf{x}) = 43$ , and the compliance is  $C(\mathbf{x}) = 958$ . The objective of compliance and volume product is  $S(\mathbf{x}) = 41,469$ , which is marked 'g' in Fig. 13. The value of the objective function  $S(\mathbf{x})$  is slightly lower than for the design of Fig. 8 using the original initial design domain.

Figure 13 shows the iteration history for  $S(\mathbf{x})$  and volume  $V(\mathbf{x})$ . The path of the objective function is smooth until 'h' when the S-history single-run-global minimum is achieved. This design at 'h' is similar to Fig. 10 with a high volume of  $V(\mathbf{x}) = 111$ ,  $C(\mathbf{x}) = 355$  and  $S(\mathbf{x}) = 39,543$ . The volume then continues to decrease as elements continue to be removed, thus, producing the S-history local minimum at 'g'.

It is observed that designs of ESO are dependent on the mesh size and the numerical singularities caused by the severe complete removal strategy of ESO. If an appropriate mesh is used, then ESO obtains topological consistent solutions with a grillage-like configuration and is, therefore, not dependent on the initial design domain.

## 5 Application of SIMP

As a comparison to ESO, we now apply SIMP to both the original initial design domain and the rectangular initial design domain. SIMP is also implemented using these two design domains with finer computational meshes. SIMP is applied using the MMA algorithm



**Fig. 14** Solution obtained by SIMP with  $p = 1$ ,  $V(\mathbf{x}) = 40$ ,  $C(\mathbf{x}) = 958$  and  $S(\mathbf{x}) = 38,373$ . The compliance  $C(\mathbf{x})$  is calculated using the refined mesh of Fig. 7

and the continuation method, the initial penalisation of which is varied. In each case, SIMP is constrained to the final volume of the ESO calculations or to the tie-beam solution of Fig. 2 where appropriate.

### 5.1 Investigation of SIMP using a coarse mesh with the original initial design domain

We begin this investigation by applying SIMP to the original coarse initial design domain of Fig. 1 using the MMA algorithm and the continuation method described in Section 2.1. Throughout this section, the convergence of  $\mathbf{x}$  measured for iteration  $k$  is defined as  $\max |\mathbf{x}_k - \mathbf{x}_{k-1}| < 0.01$ . ESO did not find a solution to this original coarse design domain, and therefore, the volume constraint of SIMP is defined as  $V(\mathbf{x}) \leq 40$  so that the solution can be compared to the tie-beam solution of Fig. 2. The filter is defined the same for ESO as  $r_{\min} = 1.05$ .

The SIMP solution to the original test problem with a coarse mesh using  $p = 1$  is given in Fig. 14 with  $C(\mathbf{x}) = 958$ , and so,  $S(\mathbf{x}) = 38,373$ . However, this solution of Fig. 14 is not discrete, and thus, has very low compliance  $C(\mathbf{x})$ , and therefore,  $S(\mathbf{x})$ . As the penalisation

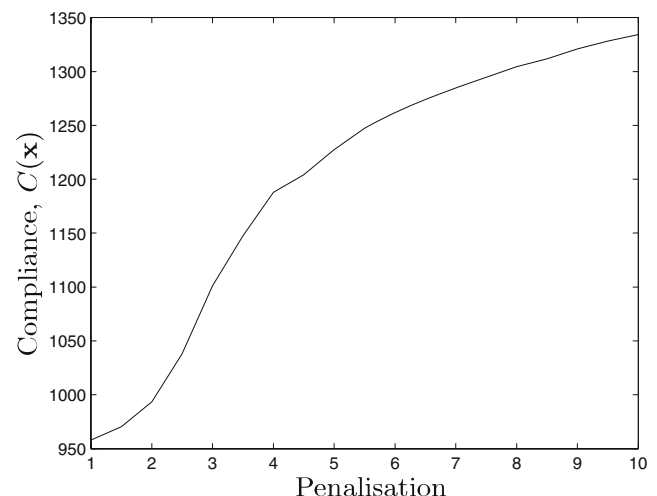


**Fig. 15** Variation of compliance  $C(\mathbf{x})$  with penalisation  $p$  when implementing the continuation method to the original coarse initial design domain of Fig. 1



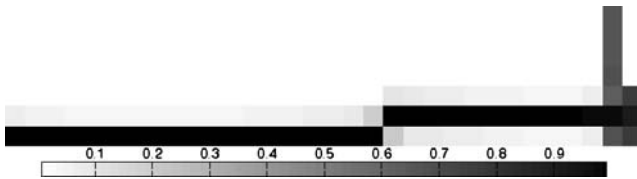


**Fig. 16** Solution of SIMP with  $p = 10$ ,  $V(\mathbf{x}) = 40$ ,  $C(\mathbf{x}) = 1,334$  and  $S(\mathbf{x}) = 53,450$ . The compliance  $C(\mathbf{x})$  is calculated using the refined mesh of Fig. 7

is increased, the solution becomes more discrete, and hence, the compliance also increases, as shown in Fig. 15.

If a penalisation of  $p > 10$  is used, the stiffness matrix  $\mathbf{K}$  becomes ill-conditioned. Thus, we choose the solution for  $p = 10$  as a sufficiently discrete solution, which, in this case, is given in Fig. 16 with  $C(\mathbf{x}) = 1,334$ , and so,  $S(\mathbf{x}) = 53,450$ . Unlike ESO, SIMP has produced a tie-beam-like solution with an equivalent volume to the tie-beam solution of Fig. 2. However, the coarse representation of the inclined main beam increases the compliance by 20% compared to the tie-beam solution of Fig. 2.

## 5.2 Investigation of SIMP using a coarse mesh with a rectangular initial design domain

We apply SIMP to the rectangular initial design domain (Fig. 4). To begin with, we specify the volume constraint as  $V(\mathbf{x}) \leq 101$  to be consistent with the result obtained using ESO in Fig. 5, and the filter as  $r_{\min} = 1.05$ . The solution obtained is illustrated in Fig. 17 with  $C(\mathbf{x}) = 385$  and  $S(\mathbf{x}) = 38,926$ , which is lower than for the original coarse design domain and the ESO solution of Fig. 5.

When we specify the volume constraint as  $V(\mathbf{x}) \leq 40$ , as it is for the tie-beam solution of Fig. 2, and a filter of  $r_{\min} = 1.05$ , application of SIMP leads to the minimum illustrated in Fig. 18 with  $C(\mathbf{x}) = 1,361$  and  $S(\mathbf{x}) = 54,703$ .

Using a rectangular initial design domain when applying SIMP yields a similar design as with the original initial design domain. Edwards et al. (2006) used a heuristic optimality criterion without continuation

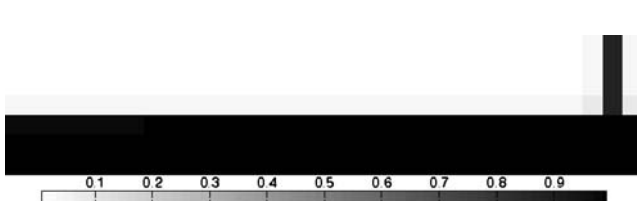


**Fig. 17** Solution obtained by SIMP with  $p = 10$ ,  $V(\mathbf{x}) = 101$ ,  $C(\mathbf{x}) = 385$  and  $S(\mathbf{x}) = 38,926$ . The compliance  $C(\mathbf{x})$  is calculated using the refined mesh of Fig. 7

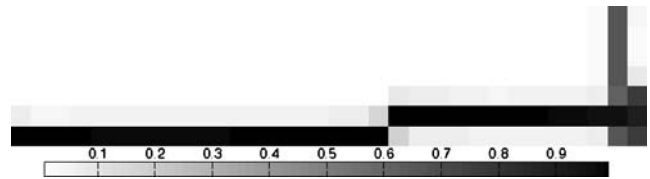


**Fig. 18** SIMP solution using a rectangular initial design domain with  $p = 10$ ,  $V(\mathbf{x}) = 40$ ,  $C(\mathbf{x}) = 1,361$  and  $S(\mathbf{x}) = 54,703$ . The compliance  $C(\mathbf{x})$  is calculated using the refined mesh of Fig. 7

and also obtained similar inclined tie-beam solutions. However, it is observed that both  $C(\mathbf{x})$  and  $S(\mathbf{x})$  are consistently higher for the inclined SIMP solutions than for the tie-beam solution of Fig. 2.

So far, we have only found local solutions that suggest there exist multiple continuation paths to different local solutions (Allgower and Georg 1990). To find a solution with lower compliance than so far obtained with SIMP and the tie-beam solution of Fig. 2, we need to explore different continuation paths. Therefore, we change the initial material layout by varying the initial penalisation  $p_{\text{init}}$  of the continuation method.

## 5.3 Investigation of initial penalisation of SIMP using the original coarse initial design domain

We now apply SIMP to the original coarse initial design domain of Fig. 1 using the continuation method but with a different initial penalisation of  $p_{\text{init}} = 1.5$ . A discrete design is still required, and so, the upper bound of  $p_{\text{upp}} = 10$  remains. Also, the penalisation power remains to be increased reasonably slowly at increments of 0.5.

The revised continuation method is applied to the original initial design domain. The volume constraint remains as  $V(\mathbf{x}) \leq 40$ , as it is for the tie-beam solution of Fig. 2, together with a filter of  $r_{\min} = 1.05$ , which is sufficient to remove checkerboard patterns. This leads to the same continuation path, and hence, inclined tie-beam solution as in the previous section (Fig. 19). This particular solution has  $C(\mathbf{x}) = 1,334$  and  $S(\mathbf{x}) = 53,450$ , which is exactly the same as that in Fig. 16.

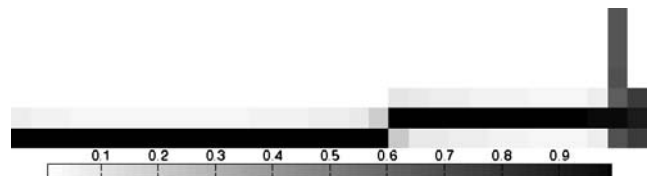


**Fig. 19** Minimum of SIMP for the coarse initial design domain using a revised initial penalisation of  $p_{\text{init}} = 1.5$ .  $p = 10$ ,  $V(\mathbf{x}) = 40$ ,  $C(\mathbf{x}) = 1,334$  and  $S(\mathbf{x}) = 53,450$ . The compliance  $C(\mathbf{x})$  is calculated using the refined mesh of Fig. 7

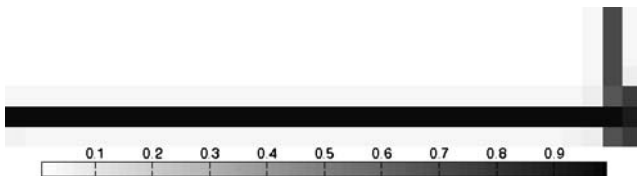


**Fig. 20** Minimum of SIMP for the coarse rectangular initial design domain using a revised initial penalisation of  $p_{\text{init}} = 1.5$ .  $p = 10$ ,  $V(\mathbf{x}) = 40$ ,  $C(\mathbf{x}) = 1,050$  and  $S(\mathbf{x}) = 42,214$ . The compliance  $C(\mathbf{x})$  is calculated using the refined mesh of Fig. 7

When the rectangular coarse initial design domain is used, however, application of SIMP leads to a new minimum (Fig. 20), which does have a horizontal main beam and a grey vertical tie.  $C(\mathbf{x}) = 1,050$  and  $S(\mathbf{x}) = 42,214$ , which are significantly lower than the solid tie-beam solution of Fig. 2 where  $C(\mathbf{x}) = 1,117$  and  $S(\mathbf{x}) = 44,684$ .

Further investigations have shown that, when higher initial penalisation values are used, SIMP is destabilised, and the solution reverts to that with an inclined main beam. In fact, only when the initial penalisation is in a small neighbourhood of  $p_{\text{init}} = 1.5$  do we obtain the horizontal main beam solution with lower compliance than the inclined tie-beam solutions and the tie-beam solution of Fig. 2.

#### 5.4 Investigation of SIMP using a refined mesh with the original initial design domain

SIMP is applied to the original initial design domain with refined mesh of Fig. 7. The volume constraint is specified as  $V(\mathbf{x}) \leq 39$  to be consistent with the ESO solution in Section 4.3, and the filter is changed to  $r_{\text{min}} = 2.5$  for the refined element size, as the element size is now much smaller.

The solution that contains an inclined main beam is illustrated in Fig. 21 with  $C(\mathbf{x}) = 1,029$  and  $S(\mathbf{x}) = 40,571$ .  $C(\mathbf{x})$  and  $S(\mathbf{x})$  are now lower than the tie-beam solution of Fig. 2, and  $S(\mathbf{x})$  is within 3% of the equivalent design from ESO presented in Fig. 8.

We now define the volume constraint to be the same as for the S-history single-run-global minimum of  $V(\mathbf{x}) \leq 99$ , which produces the solution illustrated

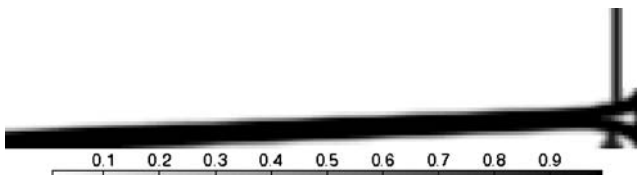


**Fig. 21** Minimum of SIMP using the refined initial design domain with  $p = 10$ ,  $V(\mathbf{x}) = 39$ ,  $C(\mathbf{x}) = 1,029$  and  $S(\mathbf{x}) = 40,571$

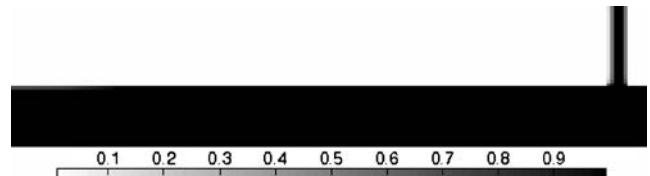


**Fig. 22** Minimum of SIMP using the refined initial design domain with  $p = 10$ ,  $V(\mathbf{x}) = 99$ ,  $C(\mathbf{x}) = 397$  and  $S(\mathbf{x}) = 39,197$

in Fig. 22. The compliance for this new solution is  $C(\mathbf{x}) = 397$  and  $S(\mathbf{x}) = 39,197$ , which, in both cases, are slightly higher than for the ESO equivalent of Fig. 10. Also, unlike the ESO equivalent solution,  $S(\mathbf{x})$  is higher for this SIMP solution than it is for the original initial design domain of Fig. 1.

The results thus far have shown that refining the mesh allows for SIMP to find smooth tie-beam-like designs with an inclined main beam when  $V(\mathbf{x}) \approx 40$  is specified. Edwards et al. (2006) also obtained inclined tie-beam solutions with low compliance when the heuristic optimality criterion was used. We now change the design domain to be rectangular and refine the mesh.

#### 5.5 Investigation of SIMP using a refined mesh with a rectangular initial design domain

SIMP is applied to the test problem with the rectangular initial design domain and a refined mesh (Fig. 11). The filter of  $r_{\text{min}} = 2.5$  for the refined element size is used with the volume constraint of  $V(\mathbf{x}) \leq 43$ , which is the same as for the equivalent ESO solution of Fig. 12. This leads to the smooth inclined design of Fig. 23 with  $C(\mathbf{x}) = 935$  and  $S(\mathbf{x}) = 40,996$ . The results are consistent with those of the original initial design domain with a fine mesh in Section 5.4.

Results similar to those of ESO are also obtained when SIMP is constrained to the higher volume of the S-history single-run-global minimum produced by ESO ( $V(\mathbf{x}) \leq 111$ ). This solution has a compliance of  $C(\mathbf{x}) = 350$  and  $S(\mathbf{x}) = 39,035$ . Therefore, SIMP also finds that the larger volume solutions have a better stiffness-volume ratio compared to the solutions with  $V(\mathbf{x}) \approx 40$ .

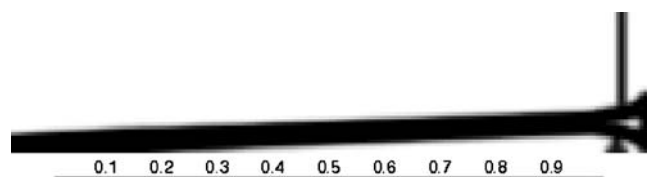


**Fig. 23** Minimum of SIMP when applied to the refined test problem with a rectangular initial design domain.  $p = 10$ ,  $V(\mathbf{x}) = 43$ ,  $C(\mathbf{x}) = 935$  and  $S(\mathbf{x}) = 40,996$

Refining the mesh for either initial design domain results in an inclined tie-beam solution when  $V(\mathbf{x}) \approx 40$  is specified. These smooth solutions then have lower compliance  $C(\mathbf{x})$  and  $S(\mathbf{x})$  compared to the tie-beam solution of Fig. 2. They are also comparable to the results from ESO (Sections 4.3 and 4.4). We note here that changing the initial penalisation of the continuation method as we did in Section 5.3 does not change the material layout of the solution. An inclined tie-beam solution is always achieved.

## 6 Conclusions

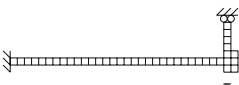







Topology optimisation methods of ESO and SIMP have been investigated using the tie-beam test problem introduced in Zhou and Rozvany (2001). ESO and SIMP were likely to encounter some difficulties because they were solving integer programming problems using heuristic algorithms based on local sensitivities.

This investigation has identified some of the difficulties associated with the two methods and the reasons behind the said difficulties. A comprehensive summary of the results is given in Table 1.

ESO and SIMP solve different optimisation problems; however, their objective functions are both based on compliance and volume. SIMP solves for a continuous minimiser, which has low compliance for a specified volume and produces a smooth solution.  $S(\mathbf{x})$  is the discrete objective function used with ESO and produces a number of minima representing a balance of compliance and volume. Given the numerical difficulties in solving such problems, both methods have been observed to perform well.

ESO failed to solve the test problem with the given coarse initial design domain. However, a simple analysis indicated that the mesh of the test problem was too coarse for further optimisation. Hence, due to the lack of termination criteria together with the severe complete element removal in the current ESO algorithm,

**Table 1** A summary of all SIMP and ESO solutions

Optimisation method and parameter	Solution		$S(\mathbf{x})$	$C(\mathbf{x})$	$V(\mathbf{x})$
Intuitive tie-beam solution (Zhou and Rozvany 2001)		(Fig. 2)	44684	1117	40
SIMP solution, original $\Omega$		(Fig. 16)	53450	1334	40
SIMP solution, rectangular $\Omega$		(Fig. 18)	54706	1361	40
SIMP solution, original $\Omega$ , $p_{init} = 1.5$		(Fig. 19)	53450	1334	40
SIMP solution, rectangular $\Omega$ , $p_{init} = 1.5$		(Fig. 20)	42214	1050	40
ESO solution, rectangular $\Omega$		(Fig. 5)	39997	396	101
SIMP solution, rectangular $\Omega$		(Fig. 17)	38926	385	101
ESO solution, refined original $\Omega^1$		(Fig. 10)	38671	392	99
SIMP solution, refined original $\Omega$		(Fig. 22)	39197	397	99
ESO solution, refined original $\Omega$		(Fig. 8)	41699	1058	39
SIMP solution, refined original $\Omega^2$		(Fig. 21)	40571	1029	39
ESO solution, refined, rectangular $\Omega$		(Fig. 12)	41469	958	43
SIMP solution, refined, rectangular $\Omega$		(Fig. 23)	40996	935	43

<sup>1</sup> Minimum  $S(\mathbf{x})$  of all solutions

<sup>2</sup> Minimum  $S(\mathbf{x})$  of all solutions with  $V(\mathbf{x}) \approx 40$

non-optimal modification in a coarse mesh environment was inevitable. This non-convergent property of ESO needs to be addressed, perhaps by an appropriate element addition algorithm.

Upon mesh refinement or the use of an enlarged initial design domain, ESO was able to find consistent topological tie-beam solutions. These tie-beam solutions of ESO had reductions in both  $S(\mathbf{x})$  and  $C(\mathbf{x})$  when compared to the tie-beam solution in Zhou and Rozvany (2001). In fact, the solution with the lowest  $S(\mathbf{x})$  was produced by ESO.

SIMP found tie-beam-like solutions when a standard continuation parameter was applied. These solutions all have inclined main beams, although the coarse mesh representation artificially increased the total compliance relative to tie-beam solution in Zhou and Rozvany (2001). Thus, it can be said that SIMP is less sensitive to the mesh size because it appears to consistently find the same inclined tie-beam solution.

SIMP has many continuation paths leading to different local solutions. This was investigated by varying the initial penalisation and the initial design domain. A different continuation path was found when the rectangular initial design domain with  $p_{\text{init}} = 1.5$  was used. This new continuation path of SIMP produced a horizontal tie-beam solution that had lower compliance than the tie-beam solution in Zhou and Rozvany (2001). Therefore, care is required when applying the continuation method with SIMP.

Using a fine computational mesh with SIMP gave tie-beam-like solutions with an inclined main beam when the volume constraint was specified as  $V(\mathbf{x}) \approx 40$ . These SIMP solutions using a refined mesh compared well with the ESO S-history local solutions also produced using a refined mesh with the same volume. The difference in  $S(\mathbf{x})$  was as close as 3% for some solutions, but SIMP produced the overall optimum.

When the volume constraint was specified as  $V(\mathbf{x}) \leq 99$  and a fine computational mesh was used, ESO and SIMP produced similar results; however, ESO produced the overall optimum solution.

**Acknowledgements** The authors thank Dr. Lars Krog, Airbus UK and Prof. Giles Hunt, University of Bath, for their useful advice and discussion. The authors would also like to thank Prof. Krister Svanberg for the MATLAB implementation of the MMA algorithm and the Numerical Analysis group at the Rutherford Appleton Lab for the FORTRAN 77 HSL package MA57. The authors acknowledge the support of UK Engineering and Physical Sciences Research Council (GR\S68477) for this research. Finally, the authors thank the anonymous referees for their inspiring and helpful comments and suggestions.

## References

- Allgower EL, Georg K (1990) Numerical continuation methods: An introduction. Springer, Berlin
- Bendsøe MP (1989) Optimal shape design as a material distribution problem. *Struct Optim* 1:193–202
- Bendsøe MP, Sigmund O (2003) Topology optimization: theory, methods and applications. Springer, Berlin
- Díaz A, Sigmund O (1995) Checkerboard patterns in layout optimization. *Struct Optim* 10:40–45
- Edwards CS, Kim H, Budd CJ (2006) Investigation on the validity of topology optimisation methods. In: 47th AIAA SDM, ASC, NDA, GSF, MDO Conference, Newport, RI, USA
- Haber RB, Jog CS, Bendsøe MP (1996) A new approach to variable topology shape design using a constraint on perimeter. *Struct Optim* 11:1–12
- Jog CS, Haber RB (1996) Stability of finite element models for distributed-parameter optimization and topology design. *Comput Methods Appl Mech Eng* 130:203–226
- Kim H, Querin OM, Steven GP, Xie YM (2000) A method for varying the number of cavities in an optimized topology using evolutionary structural optimization. *Struct Multidisc Optim* 19:140–147
- Martínez J (2005) A note on the theoretical convergence properties of the SIMP method. *Struct Multidisc Optim* 29:319–323
- Petersson J, Sigmund O (1998) Slope constrained topology optimization. *Int J Numer Methods Eng* 41:1417–1434
- Reitz A (2001) Sufficiency of a finite exponent in SIMP (power law) methods. *Struct Multidisc Optim* 21:159–163
- Rozvany GIN, Zhou M (1991) Applications of the COC method in layout optimization. In: Eschenauer H, Mattheck C, Olhoff N (eds) Proceedings of the international conference on engineering optimization in design processes, Karlsruhe, 1990. Springer, Berlin, pp 59–70
- Rozvany GIN, Zhou M, Birker T (1992) Generalized shape optimisation without homogenisation. *Struct Optim* 4:250–254
- Rutherford Appleton Laboratory (2004) Harwell subroutine library. Numerical Analysis Group. Chilton, Oxfordshire, England
- Sigmund O (1994) Design of material structures using topology optimization. PhD thesis, Technical University of Denmark
- Sigmund O (2001) A 99 line topology optimization code written in matlab. *Struct Multidisc Optim* 21:120–127
- Sigmund O, Petersson J (1998) Numerical instabilities in topology optimization: a survey on procedures dealing with checkerboards, mesh-dependencies and local minima. *Struct Optim* 16:68–75
- Svanberg K (1987) The method of moving asymptotes—a new method for structural optimization. *Int J Numer Methods Eng* 24:359–373
- Tanskanen P (2002) The evolutionary structural optimization method: theoretical aspects. *Comput Methods Appl Mech Eng* 191:5485–5498
- The Math Works (2004) MATLAB 7.0. The Math Works, Natick, MA, USA
- Xie YM, Steven GP (1993) A simple evolutionary procedure for structural optimisation. *Comput Struct* 49:885–896
- Xie YM, Steven GP (1997) Evolutionary structural optimization. Springer, Berlin
- Zhou M, Rozvany GIN (2001) On the validity of ESO type methods in topology optimization. *Struct Multidisc Optim* 21: 80–83